Separated Sonar Localization System for Indoor Robot Navigation

Wenzhou Chen , Jinhong Xu, Xiangrui Zhao, Yong Liu, *Member, IEEE*, Jian Yang

***Abstract*—This work addresses the task of mobile robot localization for indoor navigation. In this paper, we propose a novel indoor localization system based on separated sonar sensors which can be deployed in large-scale indoor environments conveniently. In our approach, the separated sonar receivers deploy on the top ceiling, and the mobile robot equipped with the separated sonar transmitters navigates in the indoor environment. The distance measurements between the receivers and the transmitters can be obtained in real-time from the control board of receivers with the infrared synchronization. The positions of the mobile robot can be computed without accumulative error. And the proposed localization method can achieve high precision in the indoor localization tasks at a very low cost. We also present a calibration method based on the simultaneous localization and mapping(SLAM) to initialize the positions of our system. To evaluate the feasibility and the dynamic accuracy of the proposed system, we construct our localization system in the Virtual Robot Experimentation Platform(V-REP) simulation platform and deploy this system in a real-world environment. Both the simulation and real-world experiments have demonstrated that our system can achieve centimeter-level accuracy. The localization accuracy of the proposed system is sufficient for robot indoor navigation.**

***Index Terms*—Localization, Navigation, Separated Sonar, SLAM.**

I. Introduction

THE high precision localization is the foundational task of mobile robot navigation. The localization research for mobile robots has received considerable attention over the past few decades [1]–[9]. The indoor environment is one of the high-profile situations for robot localization, where the GPS signals are blocked. When we consider the indoor localization problem, it is intuitive to focus on the pose accuracy of mobile robots. Additionally, as the localization system is the foundation of an indoor navigation system, both the extendibility and the cost of the system need to be concerned. However, existing localization researches mainly pay attention to the accuracy of the localization. And they can't balance the accuracy and the cost of the whole system. That hinders the development of the indoor localization systems since the practical system must make a trade-off between the accuracy and the cost.

The hardware of the localization system, also known as sensory subsystems, which provides reliable observations to estimate the position of mobile robots, has notable influence both on the accuracy and the cost. Suitable sensory subsystems are vital for the task of robot localization. The sensory subsystem can be simply divided into two classes [10], the exteroceptive and the proprioceptive types.

There are several exteroceptive sensory systems addressing the localization problems by providing external information about the environment around the robot. The pose of robots can be estimated by using external measurements from these sensory systems. The most famous research field among them is simultaneously localization and mapping(SLAM) [11]. According to the primary sensor type, the SLAM algorithm can also be divided into two classes. One is the lidar-based algorithm, another is the camera-based algorithm.

The lidar-based SLAM algorithm obtains the point cloud through the lidar sensors, and estimate the robot poses based on the point cloud map. One remarkable merit of lidar-based methods is the high precision, it can even reach the centimeter-level. There are several open-source projects like HectorSLAM [12], Cartographer [13], tinySLAM [14], etc. LOAM [15] is one of the state-of-art lidar-based SLAM algorithms, which can build the point cloud map through a signal lidar sensor. These methods perform well in their experiments, and most autonomous driving projects regard the lidar as the most important sensor in practice. However, the long-term use of the lidar-based localization system is costly. The high hardware cost and the maintenance cost is unacceptable in some industrial situations. Even the cheapest lidar is more expensive than most of the visual sensors. This character quite restricts the usage of lidar sensors in some indoor navigation tasks.

Comparing with the lidar sensors, the camera-based SLAM algorithm, also known as visual SLAM [8], [16]–[18], aims to address the SLAM tasks with visual information. This kind of algorithm utilizes all kinds of cameras, such as monocular camera [19], [20], stereo camera [21] and RGB-D camera [22], [23]. One of the famous projects in this field is the ORB-SLAM [24], [25]. ORB [26] is a kind of rotation-invariant feature descriptor. By using this kind of descriptor, the algorithm can find the feature points from the visual sensor data, and estimate the camera motions and poses. Similarly, some methods [27], [28] utilize other features such as point and line features to accomplish localization. Another similar localization method call label-based visual localization, use the specific tag to determine the pose relationships between the camera and the tag. There is no doubt that these methods have a lower economic cost than the lidar-based SLAM system. Nevertheless, the stability of camera-based SLAM algorithms are unsatisfactory, and these algorithms have considerable accumulative localization errors even with the assistance of the inertial measurement unit(IMU). The featureless surroundings

Wenzhou Chen, Jinhong Xu, Xiangrui Zhao and Yong Liu are with the Institute of Cyber-Systems and Control, Zhejiang University, Hangzhou, China, 310027, e-mail: yongliu@iipc.zju.edu.cn.

Yong Liu is the corresponding author.

and the illumination of the environment also have a great influence on the performance of visual SLAM algorithms.

Besides the aforementioned exteroceptive sensory systems, there are still some practical systems such as WiFi [2], [29]–[32], Bluetooth [3], [33], [34], Ultra-wideband(UWB) [35]–[37], QR code [38] and sonar-based methods [6], [39]–[44]. However, when we consider the robot navigation tasks in a large-scale indoor environment, the accuracy, the cost, and the extendibility should be underlined simultaneously. For instance, the UWB system has centimeter-level accuracy. But the UWB receivers need to be calibrated manually. It is a time-consuming procedure, especially for large-scale deployable systems. And the cost of the large-scale UWB system is very high. The cost of the Bluetooth system is cheap, while its localization accuracy is unacceptable in many cases. The accuracy of WiFi indoor localization systems have meter-level accuracy, which is also unacceptable in many indoor localization situations. In summary, the defects of these systems outweigh the merits. Most of them mainly consider the accuracy of localization. If we want to deploy these systems in a large-scale indoor environment, the accurate deployment of their exteroceptive sensors would be necessary. The precision of the position values influences the localization accuracy directly. For these sensory systems, it is complicated to guarantee deployment precision in practice.

The proprioceptive sensors, such as inertial measurement unit(IMU) and odometry, are widely utilized in the robot navigation system due to its ease of use and low cost. This type of sensor provides a good estimation of internal information for robot systems if given a reasonably short time interval. However, the accumulative error is a considerable shortage of proprioceptive sensors. To reduce the errors produced by proprioceptive sensors, several efforts have been presented [45]–[47].

In this paper, we present a novel localization system with separated sonar sensors. We also propose a SLAM-based calibration method to initialize the system. This study considers how separated sonar localization system can be used to provide an accurate position of a moving robot. We design a reliable hardware subsystem based on the well-designed separated sonar sensors. One of the notable shortages of exteroceptive sensory systems is the tedious process of the deployment. To address this shortage and utilize the high accuracy advantage of the lidar-based SLAM system, our approach paves the way for applying SLAM algorithms to assist the initialization of the separated sonar localization system. Furthermore, our localization system is not as susceptible to dynamic environments as the SLAM systems since our system computes the high precision position values only rely on the positions of separated sonar receivers. And the positions of separated sonar receivers are fixed after the calibration. So as long as the positions of separated sonar receivers are fixed, the dynamic environment like the furniture moving or pedestrians walking can't influence the localization accuracy. The proposed system can implement localization tasks only through the separated sonar system. Since this work just uses the SLAM system in the system initialization, we can maintain the separated sonar localization system at a very low cost.

There are lots of cases to utilize our separated sonar localization system. Such as the supermarkets, airports, shopping center, and department stores, where the QR codes can not be densely deployed and the visual recognition is easy to fail due to the complex illumination. In these situations, the sonar receivers can be deployed sparsely in the top ceiling. Even if there are some pedestrians near the mobile robot, the proposed system can still receive enough infrared signals and ultrasonic signals to provide a reliable localization service. Based on the SLAM based calibration method, the deployment of our system is also convenient.

The main contributions of this paper can be presented as follows:

1) A high precision indoor localization system is designed. The system is convenient to be deployed in a large-scale indoor environment at a very low cost.
2) A novelty convenient calibration method is presented to initialize the localization system in a large-scale environment. The extension for a larger scene is also available.
3) The localization system can work in real-time without accumulative localization error.
4) Each part of the localization system is independent, and the modules of the separated sonar system can be easily replaced.

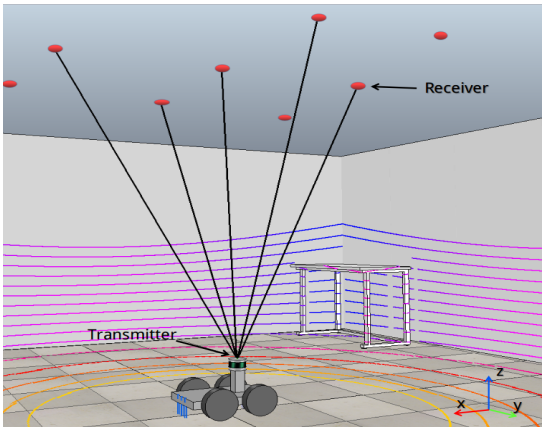

Fig. 1: The brief overview of proposed separated sonar localization system. The mobile robot equipped with the separated sonar transmitter and the lidar moves on the floor, and the separated sonar receivers are deployed on the top ceiling. The lidar sensor only utilize in the system initialization, and the system implements the localization tasks only based on the separated sonar sensors.

The rest of the paper is organized as follows. Section II focus on the method of this paper. The hardware components of the separated sonar system are introduced. The algorithms for initializing the whole system and addressing the localization tasks are designed separately. Section III presents the experiment results, and we demonstrate the proposed method both in the real-world indoor environment and the simulation platform. And Section IV presents the conclusion.

This article has been accepted for publication in a future issue of this journal, but has not been fully edited. Content may change prior to final publication. Citation information: DOI 10.1109/TIE.2020.2994856, IEEE Transactions on Industrial Electronics

II. Method

In this paper, we propose a robot localization system based on the separated sonar sensors. There are two basic foundations of the sonar-based localization system. One is the distance measurement, which can be obtained by the time-of-flight(TOF). The other is the clock synchronization for every sonar sensor. The traditional sonar-based localization systems get the distance measurements mainly through the integrated sonar sensors, which embed the sonar receiver and transmitter into one sensor. This kind of sonar sensor obtains the distance measurements by the reflection of the ultrasonic signals. But the noise wave reflection of the ultrasonic signals can easily affect the accuracy of distance measurements.

To address this issue, the proposed system utilizes the separated sonar sensor to get more reliable distance measurements. The separated sonar transmitter transmits the ultrasonic signals, and the separated sonar receivers deployed in the environment receive the signals from the transmitter. As shown in the Fig.1, the separated sonar receivers deployed on the top ceiling are illustrated by the red points, and the black lines represent the sonar signals, the ultrasonic signal from transmitter received by 5 sonar receivers at the same time. Each separate sonar has its own perceptual range. When a mobile robot equipped with a separate sonar transmitter runs on the floor, the separated sonar receivers deployed on the top ceiling can receive ultrasonic signals. The distances between nearby sonar receivers depend on the height of the top ceiling. In the perceptual range of the sonar receiver, the distances between nearby receivers increase with the rise of the top ceiling. And the trajectory of the mobile robot determines which sonar receiver can get the ultrasonic signals. As long as the sonar transmitter is covered by at least 4 receivers during working, the localization system can provide reliable position estimations. To ensure the separated sonar receivers recording the distance measurements simultaneously, our proposed system uses the infrared signals to obtain the clock synchronization. After recording several measurements, the localization algorithm can easily compute the relative position at each timestep.

The proposed separated sonar localization system can be decomposed into several parts: The hardware components of the localization system, the calibration stage of system initialization and the system localization stage. In this section, the details of these parts will be presented one by one.

A. System Components

Our indoor localization system has three different hardware components: the separated sonar receiver, the separated sonar transmitter and the control board of the separated sonar receivers. We designed the whole hardware of our localization system except for the Zigbee communication module. In this section, a brief exposition of the separated sonar localization system is presented.

When the separated sonar localization system is working, the separated sonar transmitter will send the infrared signals and the ultrasonic signals into space. If the separated sonar receivers deployed on the top ceiling get the infrared signal,

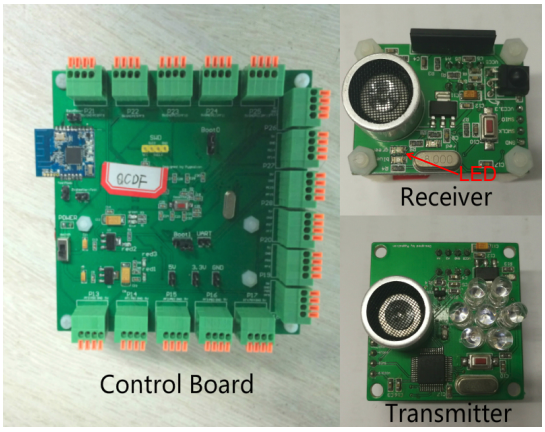

Fig. 2: The modules of separated sonar localization system.

the Microprogrammed Control Unit(MCU) embedded in the receiver will start the timer. In the exteroceptive sensory systems, the time synchronization for distributed sensors is a considerable issue. The proposed localization system assumes that the velocity of the infrared signals equals the speed of light. So when the receivers get the ultrasonic signals, they will stop the timer and send the time of flight(TOF) values to the control board in the form of level signals. As long as there is no stable infrared interference and ultrasonic noise in the indoor localization environment of the mobile robot, our separated sonar sensors can work effectively. The modules of the separated sonar transmitter and receiver are shown in Fig.2.

The most important characteristics of the control board are the real-time capability. Inspired by the logic analyzer, we developed a pseudo-logic analyzer algorithm. The algorithm divides the working sequence of the control board into three stages: The idle stage, the work stage, and the transmission stage. After initializing the control board, the MCU scans the level signal of I/O ports and waits for the rising edge during the idle stage. When one of the ports gets the rising edge, the control board transfers into the work stage. The MCU will record the level signals of each port, pack them during the work stage and transfer into the transmission stage. Based on the pseudo-logic analyzer algorithm, our hardware system can efficiently collect and transmit the data in real-time. The control board with the Zigbee communication module is shown in Fig.2.

In the hardware system, the separated sonar transmitter determines the working frequency of the system. The separated sonar receiver obtains the signal and transmits it to the control board. The pseudo-logic analyzer algorithm guarantees the stability of the hardware system. The control board will execute the localization algorithm and send the position values to the mobile robot in real-time.

B. SLAM-based Calibration

When we talk about the sonar localization system, the first important task is the sonar array deployment. In other words, the accuracy of the sonar array deployment determines the precision of the whole localization system. If we ignore the

small error during the sonar array deployment, it will be amplified in the localization stage. The error will influence the whole localization system and cause the bad performance of the localization because the initial position of sonar array is the basis of all the localization operation. In the traditional sonar-based localization system, the accurate deployment of the sonar sensor is a very difficult and tedious task, which limits the application of the sonar-based localization system. However, most of the traditional sonar-based localization systems care less about the deployment convenience and calibrate the sensors manually. Since these systems mainly focus on the localization accuracy in different situations. They pay more attention to the theoretical feasibility of their work. The deployment convenience and the extendibility are ignored naturally. Nevertheless, the aforementioned two characters are essential for practical usage. If we want to deploy the whole system in large scale indoor environments, it is difficult to accept the manual calibration process. To address this problem, we propose the SLAM-based algorithm to simplify the system's initialization task.

In the proposed localization system, we consider the Normal Distributions Transform(NDT) [48] algorithm to accomplish the system calibration task. The NDT is a kind of lidar-based SLAM algorithm commonly used in practical projects with centimeter-level accuracy. Similar to a spacial occupancy grid, the NDT algorithm subdivides the space into cells. To each cell, the algorithm assigns a normal distribution, which locally models the probability of measuring a point. The $\boldsymbol{x}_{k=1,...,m}$ are the position measurements of the reference scan points contained in the cell.

In our calibration stage, the input of the NDT algorithm is the 3D point cloud obtained by the lidar sensor. To compute the transformation relationship between each adjacent lidar frame, the NDT algorithm transforms one of them and evaluates the transformation by a score function. The score function can be formulated as Eq.1. By optimizing the score function, the optimal transformation parameter $\boldsymbol{p}$ can be iteratively computed. And that's the optimal pose estimation.

$$s(\boldsymbol{p}) = -\sum_{k=1}^{n} p(T(\boldsymbol{p}, \boldsymbol{x_k})) \tag{1}$$

Our system assumes the mobile robot is idle in the beginning, it will merge the first 10 frames as the initial global map. According to the global poses, the currently obtained laser frame will be transformed into the global coordinate system with the 100 frames interval, and it will be added to the global map. Here we just use the lidar odometry information to update the global map without loop closing optimization, for the experiment environment is a small indoor scene. If we use this system in a large-scale indoor environment, the loop closing optimization is necessary. During the calibration stage, the calibration algorithm will save the robot pose information and the separated sonar distance measurements. The robot pose information can be obtained through any high precision SLAM system. Then, the global positions of separated sonar receivers can be calculated by the Ceres optimization library [49].

We deploy k groups of separated sonar receivers in the indoor environment. There are 16 separated sonar receivers in each group. The position of the n^{th} separated sonar receiver of k^{th} group is noted as $Rev_{(k,n)}(x_{r(k,n)}, y_{r(k,n)}, z_{r(k,n)})$, where $n \in \{1,2,3,...,16\}$. The mobile robot carries the separated sonar transmitter moving horizontally in the area covered by the perceptual ranges of separated sonar receivers. We name it as localization unit. The poses of the localization unit can be obtained by the aforementioned NDT algorithm or any other SLAM system with high precision. When the localization unit transmits the ultrasonic signals, the sonar receivers will get the distance measurements. The position of the localization unit can be noted as $PoseM^{(i)}_{(k,n)}(x^{(i)}_{(k,n)}, y^{(i)}_{(k,n)}, z^{(i)}_{(k,n)})$, $i = 0,1,2,3,...,m$, where the term i represents the number of distance measurements.

When the localization unit is moving, the separated sonar receivers can get the distance measurements $l^{(i)}_{(k,n)}$ between $PoseM^{(i)}_{(k,n)}$ and $Rev_{(k,n)}$. Each robot pose is corresponding to a group of separated sonar distance measurements. And the separated sonar control board connect to the LAN of our laboratory can transmit the data via Zigbee communication module. For that reason, the system can collect the distance measurements with relative pose data in real-time, and compute the positions of sonar receivers by utilizing the Ceres optimization library. The proposed method is defined in Eq.2. We simplify the $l^{(i)}_{(k,n)}, x^{(i)}_{(k,n)}, y^{(i)}_{(k,n)}, z^{(i)}_{(k,n)}, x_{r(k,n)}, y_{r(k,n)}, z_{r(k,n)}$ terms to $l^{(i)}, x^{(i)}, y^{(i)}, z^{(i)}, x_r, y_r, z_r$. Then the position of each sonar receiver will be obtained by the Ceres optimization solver.

$$\min \sum_{i=1}^{m} (l^{(i)} - \sqrt{(x^{(i)} - x_r)^2 + (y^{(i)} - y_r)^2 + (z^{(i)} - z_r)^2})^2 \tag{2}$$

C. System Localization Method

In the localization stage, the separated sonar localization system localizes the mobile robot based on the positions of sonar receivers obtained in the calibration stage. When the system captures at least four distance measurements, it can simply compute the position of the localization unit with separated sonar sensors. So in this section, we will analyze the four points localization case as an example. And it can easily extend to other multiple points localization cases, as we illustrated in the experiments section.

We assume there are four separated sonar receivers deployed on the ceiling. Their positions are noted as $P_1(x_1, y_1, z_1)$, $P_2(x_2, y_2, z_2)$, $P_3(x_3, y_3, z_3)$, $P_4(x_4, y_4, z_4)$. To distinguish the notations from last section, we use d_n to represent the distance measurements between localization unit and the sonar receivers, where $n = 1,2,3,4$. Our goal is obtaining the position $Q(x, y, z)$ of localization unit carried by the mobile robot. As shown in the Eq.3, the ρ term represents the systematic uncertainty and the ranging uncertainty.

$$\begin{gathered} \sqrt{(x - x_i)^2 + (y - y_i)^2 + (z - z_i)^2} - d_i + \rho_i = 0 \\ where\ i = 1,2,3,4. \end{gathered} \tag{3}$$

To simplify the equation and get its solution, the Eq.3 can be rewritten to a local linearization form, as shown in the Eq.4.

This article has been accepted for publication in a future issue of this journal, but has not been fully edited. Content may change prior to final publication. Citation information: DOI 10.1109/TIE.2020.2994856, IEEE Transactions on Industrial Electronics

The g term is the gradient of the nonlinear equation shown in the Eq.5.

$$f_k(x_0,y_0,z_0)+(x-x_0)g_{k1}+(y-y_0)g_{k2}+(z-z_0)g_{k3}=0 \quad where\ k=1,2,3,4. \tag{4}$$

$$g_{k1}=\frac{\partial f_k}{\partial x}|_{(x_0,y_0,z_0)}\ ,g_{k2}=\frac{\partial f_k}{\partial y}|_{(x_0,y_0,z_0)}\ ,g_{k3}=\frac{\partial f_k}{\partial z}|_{(x_0,y_0,z_0)} \tag{5}$$

Now, we can reformulate the problem in a more concise form, as shown in the Eq.6. The problem is changed into solving the linear overdetermined equation. Then, the position value will be obtained by the iteration form Eq.7.

$$\boldsymbol{G_0}\begin{bmatrix}x-x_0\\y-y_0\\z-z_0\end{bmatrix}=-\boldsymbol{F_0} \tag{6}$$

$$where\ \boldsymbol{G_0}=[g_{ij}],\ \boldsymbol{F_0}=f_i(x_0,y_0,z_0)\ (i,j,k=1,2,3,4.)$$

$$\begin{bmatrix}x_{k+1}\\y_{k+1}\\z_{k+1}\end{bmatrix}=\begin{bmatrix}x_k\\y_k\\z_k\end{bmatrix}-(\boldsymbol{G_k^T}\boldsymbol{G_k})^{-1}\boldsymbol{G_k^T}\boldsymbol{F_k} \tag{7}$$

$$where\ k=0,1,2,...$$

When the separated sonar localization system is working, the computer will load m distance measurements. During the movement, distance measurements and the location values from relative sonar receivers will be saved in real-time. The position of the mobile robot can be computed 20 times per second, for the system frequency is 20Hz.

III. Experiments

To evaluate the performance of our separated sonar localization system, sufficient experiments are illustrated in both simulation platform and real-world environment. To construct the whole localization system, the simulation is built by a robot simulator named Virtual Robot Experimentation Platform(V-REP), which is used for fast modeling and validating the proposed localization system. After examing the localization system in the simulation environment, we also implement the whole localization system in our laboratory. As shown in Fig.3(a), the mobile robot equipped with the lidar sensor and the separated sonar transmitter is the localization unit. In this section, the details of the simulation results and the real-world experiments will be introduced clearly.

A. Localization Simulation

To validate the proposed localization method and precisely analyze the localization errors, we build the whole localization system in the Virtual Robot Experimentation Platform (V-REP) environment. In this simulation environment, the ground truth position of objects can be easily obtained. It can be directly utilized in the dynamic accuracy analysis of the proposed separated sonar localization system.

In the V-REP simulation environment, we build an indoor scene to simulate our laboratory. As shown in the Fig.3(b), the small room has a transparent ceiling with some furniture and plants in the corner. The mobile robot equipped with the lidar sensor and the separated sonar transmitter runs on the floor. The separated sonar receivers deployed on the ceiling are invisible unless they receive the sonar signals from the separated transmitter. There are 25 separated sonar receivers on the ceiling. The detection distance of each sonar is $5m$, and the detection angle of each one is $45°$. These two parameters are determined by the measurements of our separated sonar receivers and the transmitter.

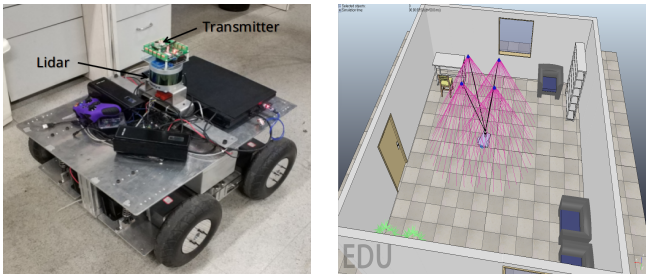

(a) (b)

Fig. 3: (a) The localization unit. (b) The simulation of robot localization. The figure only shows separated sonar receivers in working state. The receivers in idle states are invisible.

When the mobile robot moves in the room, the sonar receivers would get the distance measurements. Then the calibration algorithm can get the position estimations of the separated sonar receivers on the ceiling, and initialize their spacial positions. At the localization stage, the system addresses the localization task depending on these position initializations.

In order to authentically simulate the actual situation in practice, some noise is added to the simulation system. Before adding the noise, the hardware properties of both separated sonar receivers and the transmitter are fully tested. By analyzing the distance error measurements, the distance error of our separated sonar modules is less than $4cm$ in their valid working range. To get the accuracy lower bound of the proposed system, we add the random noise in the distance measurements with the amplitude of $4cm$. Furthermore, since the lidar sensor in the simulation environment has better accuracy than the real lidar, we add the random noise in the calibration results with the positive-negative amplitude from $0cm$ to $5cm$. To compare the results with the positive-negative case, we also add the random noise with a positive amplitude from $0cm$ to $5cm$.

After adding the noise, we run our simulation system, record the measurements and compute the position of the localization unit in real-time. The dynamic accuracy analysis of the proposed localization system is shown in Fig.4, we plot the absolute trajectory errors separately in 3-axes. To illustrate the position errors more clearly, we draw the absolute trajectory error diagram with 5 frames interval. The abscissa represents the number of location points. In other words, the number means the time step in the trajectory. And the ordinate values express the absolute trajectory errors.

As shown in the Fig.5, we also draw the root mean square error(RMSE) diagram of the trajectory estimation. The root

This article has been accepted for publication in a future issue of this journal, but has not been fully edited. Content may change prior to final publication. Citation information: DOI 10.1109/TIE.2020.2994856, IEEE Transactions on Industrial Electronics

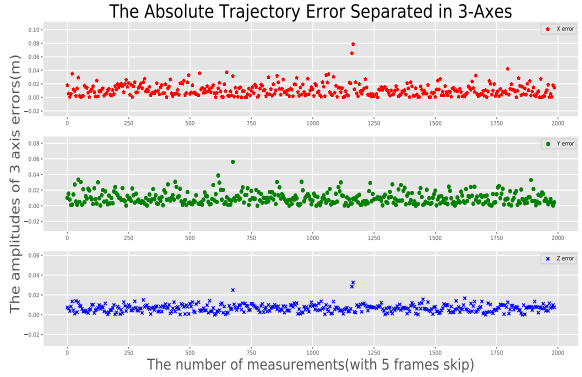

Fig. 4: One of the absolute trajectory errors in 3 axes with 5 frames interval. In this case, we add the random noise in the distance measurements with the amplitude of $4cm$. And we also add the positive-negative random noise in the calibration results with the range of $4cm$.

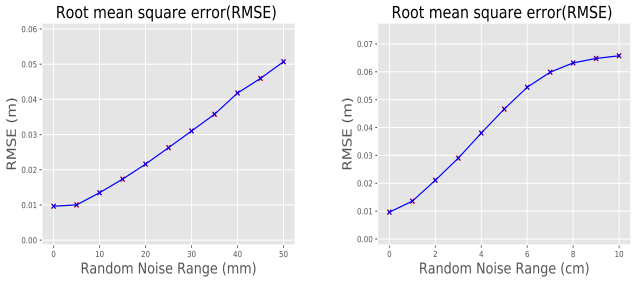

Fig. 5: The RMSE curve of trajectory. The left diagram is the RMSE curve with positive random noise, the amplitude of noise starts from $0cm$ to $5cm$ with the $0.5cm$ interval. The RMSE curve in right diagram has the amplitude starts from $0cm$ to $10cm$ with $1cm$ interval, and the noise has a $-5cm$ shift.

mean square error(RMSE) is given by Eq.8, where the x_k represents the estimated position of the mobile robot and the $k(k = 1,2,...,N)$ means the k^{th} independent measurements data. x represents the real position of the robot. N is the number of total measurements.

$$RMSE = \sqrt{\frac{1}{N}\sum_{k=1}^{N}(\boldsymbol{x}-\boldsymbol{x_k})^2} \tag{8}$$

The diagrams show that the root mean square error of the estimation trajectory is less than $7cm$, even though we add the random noise with a positive-negative amplitude of $5cm$. Generally, the range of random noise is less than $4cm$ in practical lidar-based SLAM systems. So we can infer that the localization error of our system is about $5cm$. Thus, the proposed separated sonar localization system has centimeter-level accuracy.

B. real-world Calibration

In the real-world experiments, we use the SLAM-based algorithm to initialize the whole separated sonar localization system deployed on the ceiling in our laboratory. As shown in the Fig.6(a), each separated sonar receiver is illustrated by a high light LED. The blink mode of LED can express the different working states of each receiver. When the localization unit moves on the ground, we can easily recognize which separated sonar receiver is working properly. However, in the real-world environment, it is hard to get the ground truth position values to analyze the calibration performance of our method. To evaluate the accuracy of the SLAM-based algorithm ingeniously, we present a kind of grid point based calibration method. The experiment results of the grid point based calibration method are regarded as the ground truth position of the separated sonar receivers.

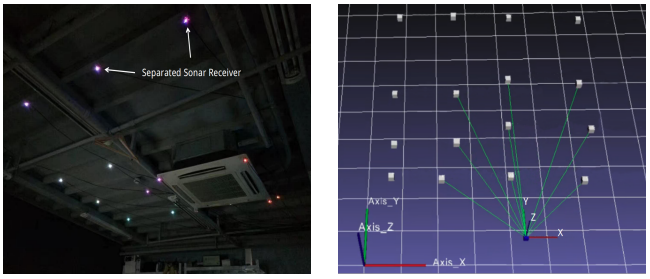

(a) (b)

Fig. 6: (a) The environment of real world experiments: the luminous points represent the separated sonar receivers. When they get the signals, the constant light will change to flashing. (b) The visualization of real world localization experiment.

1) SLAM-based Calibration: In the SLAM-based calibration experiment, we remotely control the mobile robot to move in the laboratory. The mobile robot equipped with the lidar sensor and the sonar transmitter moves along the preset trajectory. The computer in the mobile robot will save the lidar data. The point cloud map of the laboratory can be obtained by replaying the collected lidar data. By using the aforementioned calibration method, we can easily get the positions of separated sonar receivers.

We can also compute the accurate pose matrix through the point cloud map. As shown in Fig.7, the red line is the route of the mobile robot and the blue part of the point cloud map is the wall of our laboratory, the green part of point cloud map mainly represents the desks and chairs in our laboratory. To evaluate the performance, we amplify part of the point cloud map which represents the wall. The approximate measurements can be obtained through the point cloud visualization and the thickness of the wall is less than 1cm. If the point cloud map is absolutely unbiased, the thickness should be 0 cm. So we can roughly infer that the reconstruction accuracy is less than 1 cm. And the accuracy of the SLAM-based calibration method is in the centimeter-level.

2) Grid Point Based Calibration: The accuracy evaluation through point cloud visualization is an intuitive but deficient way. When we consider evaluating the performance of real-

This article has been accepted for publication in a future issue of this journal, but has not been fully edited. Content may change prior to final publication. Citation information: DOI 10.1109/TIE.2020.2994856, IEEE Transactions on Industrial Electronics

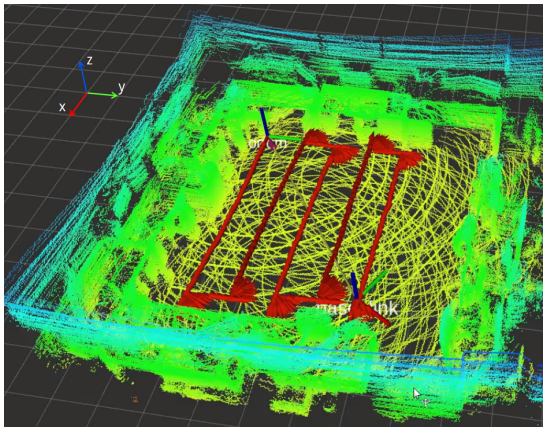

Fig. 7: The point cloud map of laboratory. The red line shows the trajectory of the mobile robot. The green, yellow and blue points construct the point cloud map of laboratory.

world localization system, one of the most difficult problems is getting the ground truth positions of all the separated sonar receivers deployed on the ceiling. To address this issue, we add the grid point based calibration experiments. By assuming all the ground tiles have the same standard size, the tile grid intersections construct the grid points. One of the grid points is defined as the origin of the global coordinate system. The ground tile is a standard square with a side of 60 cm. We deployed the separated sonar transmitter on the intersections. Getting the distance measurements between the transmitter and receivers, recording the relative positions of separated sonar transmitter. Depending on the measurement collection, the positions of separated sonar receivers can be easily computed.

3) Error Analysis: In the real-world calibration experiments, the grid point based calibration experiments and the SLAM-based calibration experiments utilize different coordinate systems. The origin of SLAM-based calibration experiments is in the localization unit, which we call the mobile robot coordinate system. The coordinate system used in the grid point based calibration experiments is straightly defined as the global coordinate system. The link between them is a transformation matrix T_G^S. By regarding the grid point based calibration results as ground truth positions, we can compute the transformation matrix and analyze the calibration accuracy.

Based on the experiment results, the iterative closest points(ICP) [50] method could compute the transformation matrix T_G^S. Then, we can align the mobile robot coordinate system and the global coordinate system through the transformation matrix, evaluate the SLAM-based calibration results by utilizing the transformation matrix. The comparisons between the SLAM-based calibration experiments and the grid point based calibration experiments are listed on the Table I, and the mean square error equals to $0.039m$. So we can indicate that the SLAM-based calibration method has centimeter-level calibration accuracy. Here we only list 16 calibration results of separated sonar receivers as an example. When the proposed localization system deployed in practice, it is convenient to increase the number of receivers and expand the system deployment in large scale indoor environment. Increasing the number of separated sonar receivers can also reduce the negative impact of some outliers and improve the accuracy of the transformation matrix according to the principle of ICP method.

C. real-world Localization

In this section, the details of real-world localization experiments will be discussed. We also compare our system with some famous SLAM algorithms. And the performance of the proposed separated sonar localization system deployed in our laboratory will be analyzed elaborately.

In the real-world localization experiments, we visualize the separated sonar receivers and the localization unit in real-time based on the OpenCV library. As shown in the Fig.6(b), the cubes in grey color are the separated sonar receivers. To concisely illustrate the spacial relationship, the ceiling is omitted like any other unconcerned objects in our laboratory. The small coordinate axes connect to the cubes with green line represents the localization unit. The green connection lines mean that these cubes have received the valid sonar signals from the separated sonar transmitter. The big coordinate axes on the left bottom is at the origin of the global coordinate system.

By running the localization system and the visualization program, we can stably get the position value of the localization unit, and observe its movement on the screen in real-time. However, getting the ground truth position of the localization unit is still impossible. It's hard to evaluate the accuracy of our separated sonar localization system without the ground truth. So we figure out two ways to address this issue.

1) Static Localization: In the previous section, we have assumed that all the grid points have the same size. The aforementioned grid point coordinate system is chosen as the global coordinate system again. When we put the localization unit on the intersections, its position value can be regarded as ground truth position. Since the algorithm needs enough valid measurements to compute the positions, the localization unit should at least be covered by 4 different separated sonar receivers. The grid point intersections on the edge of the sonar array lacking the signal coverage wouldn't be considered. We finally choose 15 intersections as test locations. At each test location, approximately 10 seconds of measurements are collected.

To evaluate the accuracy of static localization, the proposed separated sonar localization system should be tested as an integrated system. The positions of separated sonar receivers are initialized by the experiment results obtained at the calibration stage. In this part of the experiment, we separately utilize the grid point based calibration results and the SLAM-based calibration results. When we use the grid point based calibration results, the localization stage, and the calibration stage both work on the global coordinate system. However, if we use the SLAM-based calibration results, the positions of separated sonar receivers need to be transformed into the global coordinate system. The transformation matrix T_G^S is computed in the previous section. In our experiments, even if we only deploy 16 sonar receivers on the ceiling, the

This article has been accepted for publication in a future issue of this journal, but has not been fully edited. Content may change prior to final publication. Citation information: DOI 10.1109/TIE.2020.2994856, IEEE Transactions on Industrial Electronics

TABLE I: The calibration experiment results comparison of sonar sensor deployments. The Xs, Ys, Zs values are the experiment results of the SLAM-based calibration, and the Xg, Yg, Zg values are the grid point based calibration results.

ID	1	2	3	4	5	6	7	8	9	10	11	12	13	14	15	16
$Xs(m)$	0.52	0.52	1.46	1.44	0.52	1.22	2.17	3.16	2.20	3.42	2.26	3.32	0.57	1.45	2.32	3.30
$Xg(m)$	0.51	0.53	1.45	1.49	0.53	1.26	2.19	3.18	2.20	3.39	2.21	3.28	0.53	1.38	2.25	3.25
$\Delta X(m)$	0.01	0.01	0.01	0.05	0.01	0.04	0.02	0.02	0.00	0.03	0.05	0.04	0.04	0.07	0.07	0.05
$Ys(m)$	1.12	2.10	1.13	2.16	0.36	0.32	0.36	0.29	1.18	1.14	2.03	2.01	3.29	3.34	3.29	3.28
$Yg(m)$	1.18	2.13	1.18	2.17	0.37	0.37	0.37	0.36	1.24	1.23	2.07	2.08	3.32	3.35	3.38	3.31
$\Delta Y(m)$	0.06	0.03	0.05	0.01	0.01	0.05	0.01	0.07	0.06	0.09	0.04	0.07	0.03	0.01	0.09	0.03
$Zs(m)$	2.15	2.16	2.16	2.17	2.46	2.46	2.48	2.48	2.48	2.44	2.49	2.48	2.48	2.48	2.52	2.47
$Zg(m)$	2.15	2.17	2.16	2.16	2.47	2.46	2.46	2.45	2.47	2.50	2.47	2.44	2.46	2.46	2.44	2.45
$\Delta Z(m)$	0.00	0.01	0.00	0.01	0.01	0.00	0.02	0.03	0.01	0.06	0.02	0.04	0.02	0.02	0.08	0.02

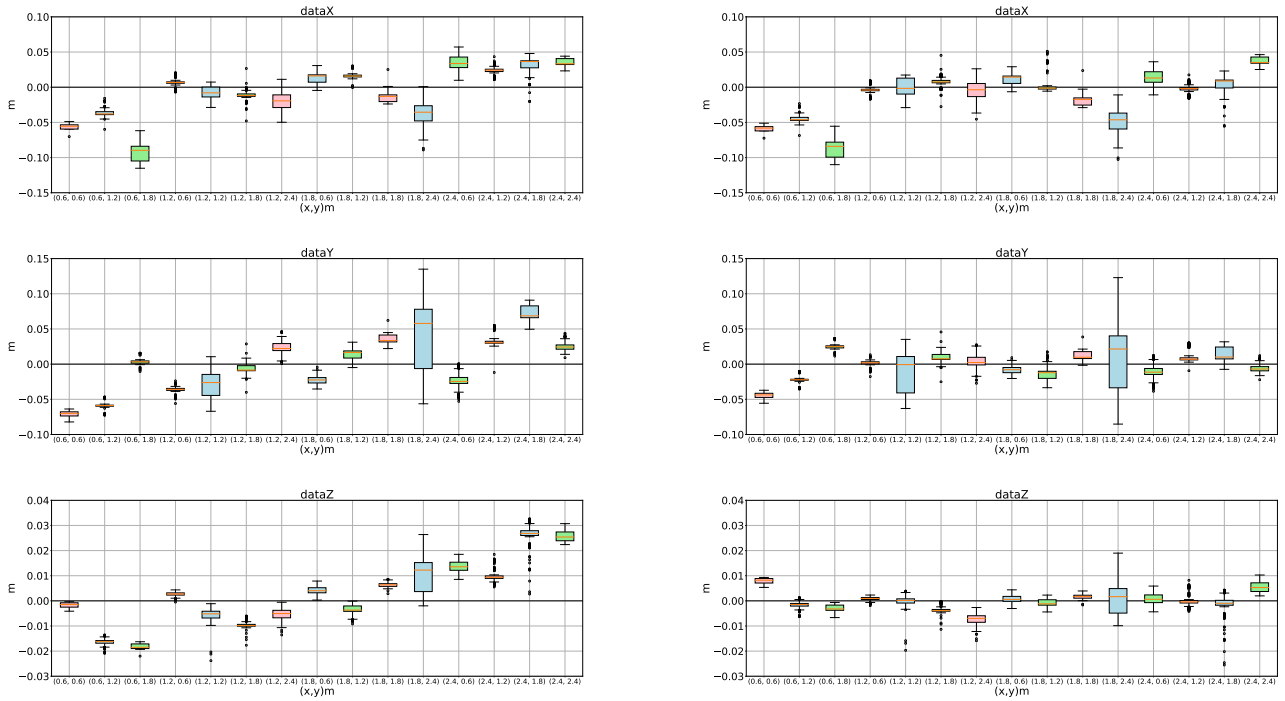

Fig. 8: The left column shows the localization errors in 3 axes with respect to the SLAM-based calibration results, and the right column shows the localization errors with respect to the ground tile based calibration results.

localization system performs well and reaches a high-level accuracy. As shown in Fig.8, the box-and-whisker diagrams of two localization experiments illustrate the statistical properties of the localization errors. The left three diagrams are the localization errors of three axes in the SLAM-based localization experiments. The right ones are the results of the grid point localization experiments.

2) Dynamic Localization: After evaluating the static localization accuracy, we additionally utilize the Optitrack Motion Tracker system to exam the dynamic localization accuracy of our system. As shown in the Fig.9(a), the OptiTrack Motion Tracker system provides the ground truth and the proposed separates sonar localization system generates the measurements of the position values. The experimental area is surrounded by 16 Flex13 cameras of the Optitrack Motion Tracker system. The frame rate of the Flex13 camera is 120 fps, and its resolution is 1.3 megapixel (1280*1024). These features enable us to capture ground truth data with a precision down to 0.5 mm, making the ground truth very accurate and reliable. The software we use in the OptiTrack system is Motive 2.1 optical motion capture software. The separated sonar receivers are deployed on the blackboard. The separated sonar receivers and the transmitters are carefully calibrated by the OptiTrack system. After simultaneously starting the OptiTrack system and the separated sonar system, we move the separated sonar transmitter in a spiral trajectory. The position values of the transmitter are recorded by two localization systems.

The localization trajectory of the separated sonar transmitter is shown in the Fig.9(b), The black points illustrate the sonar receivers deployed on the blackboard. Since the OptiTrack system and the separated sonar localization system have a different frequencies, we resample the ground truth data and align it with the estimation trajectory. The red points express

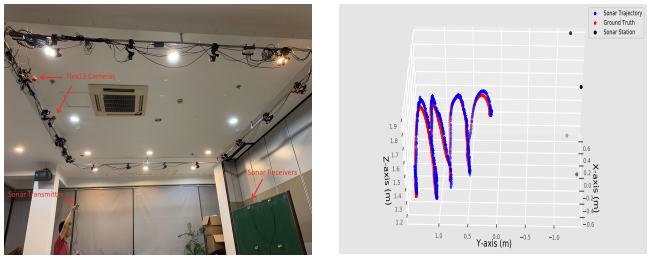

(a) (b)

Fig. 9: (a) The Optitrack Motion Tracker system. The experimental area is surrounded by 16 Flex13 cameras of the Optitrack Motion Tracker system. The frame rate of the Flex13 camera is 120 fps, and its resolution is 1.3 megapixel (1280*1024). (b) The localization trajectory of the separated sonar transmitter. The black points illustrate the sonar receivers deployed on the blackboard. The red points express the ground truth trajectory obtained by the OptiTrack system. The blue points represent the position estimation obtained by the separated sonar localization system.

the ground truth trajectory obtained by the OptiTrack system. The blue points represent the position estimation obtained by the separated sonar localization system. After the resampling and aligning, the mean absolute trajectory error(ATE) between them is $0.056m$. Compared with the simulation results in our paper, we have reason to believe that the accuracy of our separated sonar localization system is in the centimeter level.

Based on the above experiment results, we can indicate that the localization accuracy of our system can achieve the centimeter-level. As shown in Table II, we compare the mean absolute trajectory errors(ATE) of different localization systems. Such as the Stereo OV SLAM, the Stereo OV VIO, and the Stereo Basalt, etc. The localization accuracy of the separated sonar localization system can achieve the same level of precision as famous visual SLAM methods. The similar centimeter-level accuracy also proves the quality of our separated sonar localization system. Furthermore, since the localization errors of the static localization experiments and the dynamic localization experiments are both in the centimeter-level, we can infer that our separated sonar localization system can tolerate a certain degree of calibration errors. The robustness of our system is also significant to practical usages.

IV. Conclusion

In this paper, we propose a separated sonar-based localization system considering the high localization accuracy, the low cost, and the deployment convenience simultaneously, which is essential for a practical large-scale indoor localization system. Our system consists of the calibration stage for system initialization and the localization stage for general working. Our novel calibration method merges the SLAM system and the separated sonar sensors to initialize the whole localization system. After the calibration stage, the separated sonar-based localization system won't be influenced by the dynamic environment. And it can compute the high precision positions at the localization stage in real-time without the aforementioned SLAM system. The SLAM system used in the calibration stage can be replaced by most of the state-of-art SLAM systems to promote calibration quality. At the localization stage, our localization system performs well both in the simulation platform and in the real-world environment. The separated sonar sensors can obtain an accurate position of the mobile robot and work stably in real-time without accumulative error.

References

[1] L. Mainetti, L. Patrono, and I. Sergi, "A survey on indoor positioning systems," in *Software, Telecommunications and Computer Networks (SoftCOM), 2014 22nd International Conference on*. IEEE, 2014, pp. 111–120.

[2] J. Biswas and M. Veloso, "Wifi localization and navigation for autonomous indoor mobile robots," in *Robotics and Automation (ICRA), 2010 IEEE International Conference on*. IEEE, 2010, pp. 4379–4384.

[3] M. Altini, D. Brunelli, E. Farella, and L. Benini, "Bluetooth indoor localization with multiple neural networks," in *Wireless Pervasive Computing (ISWPC), 2010 5th IEEE International Symposium on*. IEEE, 2010, pp. 295–300.

[4] H.-S. Ahn and K. H. Ko, "Simple pedestrian localization algorithms based on distributed wireless sensor networks," *IEEE Transactions on Industrial Electronics*, vol. 56, no. 10, pp. 4296–4302, 2009.

[5] Y. Wang, W. Chen, J. Wang, and H. Wang, "Active global localization based on localizability for mobile robots," *Robotica*, vol. 33, no. 8, pp. 1609–1627, 2015.

[6] O. Bischoff, N. Heidmann, J. Rust, and S. Paul, "Design and implementation of an ultrasonic localization system for wireless sensor networks using angle-of-arrival and distance measurement," *Procedia Engineering*, vol. 47, pp. 953–956, 2012.

[7] A. Amanatiadis, "A multisensor indoor localization system for biped robots operating in industrial environments," *IEEE Transactions on Industrial Electronics*, vol. 63, no. 12, pp. 7597–7606, 2016.

[8] T. Taketomi, H. Uchiyama, and S. Ikeda, "Visual slam algorithms: a survey from 2010 to 2016," *IPSJ Transactions on Computer Vision and Applications*, vol. 9, no. 1, p. 16, 2017.

[9] C. Premachandra, D. Ueda, and K. Kato, "Speed-up automatic quadcopter position detection by sensing propeller rotation," *IEEE Sensors Journal*, vol. 19, no. 7, pp. 2758–2766, 2018.

[10] S. J. Kim and B. K. Kim, "Dynamic ultrasonic hybrid localization system for indoor mobile robots," *IEEE Transactions on Industrial Electronics*, vol. 60, no. 10, pp. 4562–4573, 2013.

[11] C. Cadena, L. Carlone, H. Carrillo, Y. Latif, D. Scaramuzza, J. Neira, I. Reid, and J. J. Leonard, "Past, present, and future of simultaneous localization and mapping: Toward the robust-perception age," *IEEE Transactions on Robotics*, vol. 32, no. 6, pp. 1309–1332, 2016.

[12] S. Kohlbrecher, J. Meyer, O. von Stryk, and U. Klingauf, "A flexible and scalable slam system with full 3d motion estimation," in *Proc. IEEE International Symposium on Safety, Security and Rescue Robotics (SSRR)*. IEEE, November 2011.

[13] W. Hess, D. Kohler, H. Rapp, and D. Andor, "Real-time loop closure in 2d lidar slam," in *2016 IEEE International Conference on Robotics and Automation (ICRA)*, 2016, pp. 1271–1278.

[14] B. Steux and O. El Hamzaoui, "tinyslam: A slam algorithm in less than 200 lines c-language program," in *Control Automation Robotics & Vision (ICARCV), 2010 11th International Conference on*. IEEE, 2010, pp. 1975–1979.

[15] J. Zhang and S. Singh, "LOAM: Lidar odometry and mapping in real-time," in *Robotics: Science and Systems Conference (RSS)*, Berkeley, CA, July 2014.

[16] P. Geneva, K. Eckenhoff, W. Lee, Y. Yang, and G. Huang, "Openvins: A research platform for visual-inertial estimation," in *IROS 2019 Workshop on Visual-Inertial Navigation: Challenges and Applications, Macau, China*, 2019.

[17] V. Usenko, N. Demmel, D. Schubert, J. Stückler, and D. Cremers, "Visual-inertial mapping with non-linear factor recovery," *IEEE Robotics and Automation Letters*, 2019.

[18] M. Burri, J. Nikolic, P. Gohl, T. Schneider, J. Rehder, S. Omari, M. W. Achtelik, and R. Siegwart, "The euroc micro aerial vehicle datasets," *The International Journal of Robotics Research*, 2016. [Online]. Available: http://ijr.sagepub.com/content/early/2016/01/21/0278364915620033.abstract

TABLE II: The mean absolute trajectory errors(ATE) of different localization systems. The listed SLAM methods are examed in parts of the EuROC dataset. Including the V1_01_easy, V1_02_medium, V1_03_difficult, V2_01_easy, and V2_02_medium.

	Stereo OV SLAM	Stereo OV VIO	Stereo Basalt	Mono OV SLAM	Mono OV VIO	Ours
Mean ATE(m)	0.054	0.055	0.057	0.079	0.148	0.056

[19] J. Engel, T. Schöps, and D. Cremers, "Lsd-slam: Large-scale direct monocular slam," in *European Conference on Computer Vision*. Springer, 2014, pp. 834–849.

[20] K. Wang, Y.-H. Liu, and L. Li, "A simple and parallel algorithm for real-time robot localization by fusing monocular vision and odometry/ahrs sensors," *IEEE/ASME Transactions on Mechatronics*, vol. 19, no. 4, pp. 1447–1457, 2014.

[21] I. Cvišić, J. Ćesić, I. Marković, and I. Petrović, "Soft-slam: Computationally efficient stereo visual slam for autonomous uavs," *Journal of Field Robotics*, 2017.

[22] C. Kerl, J. Sturm, and D. Cremers, "Robust odometry estimation for rgb-d cameras," in *Robotics and Automation (ICRA), 2013 IEEE International Conference on*. IEEE, 2013, pp. 3748–3754.

[23] Q. Sun, J. Yuan, X. Zhang, and F. Sun, "Rgb-d slam in indoor environments with sting-based plane feature extraction," *IEEE/ASME Transactions on Mechatronics*, vol. 23, no. 3, pp. 1071–1082, 2018.

[24] R. Mur-Artal, J. M. M. Montiel, and J. D. Tardos, "Orb-slam: a versatile and accurate monocular slam system," *IEEE Transactions on Robotics*, vol. 31, no. 5, pp. 1147–1163, 2015.

[25] R. Mur-Artal and J. D. Tardós, "Orb-slam2: An open-source slam system for monocular, stereo, and rgb-d cameras," *IEEE Transactions on Robotics*, vol. 33, no. 5, pp. 1255–1262, 2017.

[26] E. Rublee, V. Rabaud, K. Konolige, and G. Bradski, "Orb: An efficient alternative to sift or surf," in *Computer Vision (ICCV), 2011 IEEE international conference on*. IEEE, 2011, pp. 2564–2571.

[27] X. Zuo, X. Xie, Y. Liu, and G. Huang, "Robust visual slam with point and line features," in *2017 IEEE/RSJ International Conference on Intelligent Robots and Systems (IROS)*. IEEE, 2017, pp. 1775–1782.

[28] C. Premachandra, M. Murakami, R. Gohara, T. Ninomiya, and K. Kato, "Improving landmark detection accuracy for self-localization through baseboard recognition," *International Journal of Machine Learning and Cybernetics*, vol. 8, no. 6, pp. 1815–1826, 2017.

[29] Y. Sun, M. Liu, and M. Q.-H. Meng, "Wifi signal strength-based robot indoor localization," in *Information and Automation (ICIA), 2014 IEEE International Conference on*. IEEE, 2014, pp. 250–256.

[30] Z. Chen, H. Zou, H. Jiang, Q. Zhu, Y. C. Soh, and L. Xie, "Fusion of wifi, smartphone sensors and landmarks using the kalman filter for indoor localization," *Sensors*, vol. 15, no. 1, pp. 715–732, 2015.

[31] B. Benjamin, G. Erinc, and S. Carpin, "Real-time wifi localization of heterogeneous robot teams using an online random forest," *Autonomous robots*, vol. 39, no. 2, pp. 155–167, 2015.

[32] Z.-A. Deng, Y. Hu, J. Yu, and Z. Na, "Extended kalman filter for real time indoor localization by fusing wifi and smartphone inertial sensors," *Micromachines*, vol. 6, no. 4, pp. 523–543, 2015.

[33] L. Chen, H. Kuusniemi, Y. Chen, J. Liu, L. Pei, L. Ruotsalainen, and R. Chen, "Constraint kalman filter for indoor bluetooth localization," in *Signal Processing Conference (EUSIPCO), 2015 23rd European*. IEEE, 2015, pp. 1915–1919.

[34] Y. Zhuang, J. Yang, Y. Li, L. Qi, and N. El-Sheimy, "Smartphone-based indoor localization with bluetooth low energy beacons," *Sensors*, vol. 16, no. 5, p. 596, 2016.

[35] S. Gezici, Z. Tian, G. B. Giannakis, H. Kobayashi, A. F. Molisch, H. V. Poor, and Z. Sahinoglu, "Localization via ultra-wideband radios: a look at positioning aspects for future sensor networks," *IEEE signal processing magazine*, vol. 22, no. 4, pp. 70–84, 2005.

[36] B. Kempke, P. Pannuto, and P. Dutta, "Polypoint: Guiding indoor quadrotors with ultra-wideband localization," in *Proceedings of the 2nd International Workshop on Hot Topics in Wireless*. ACM, 2015, pp. 16–20.

[37] J. Tiemann, F. Eckermann, and C. Wietfeld, "Atlas-an open-source tdoa-based ultra-wideband localization system," in *Indoor Positioning and Indoor Navigation (IPIN), 2016 International Conference on*. IEEE, 2016, pp. 1–6.

[38] P. Nazemzadeh, D. Fontanelli, D. Macii, and L. Palopoli, "Indoor localization of mobile robots through qr code detection and dead reckoning data fusion," *IEEE/ASME Transactions on Mechatronics*, vol. 22, no. 6, pp. 2588–2599, 2017.

[39] N. B. Priyantha, "The cricket indoor location system," Ph.D. dissertation, Massachusetts Institute of Technology, 2005.

[40] M. Hazas and A. Hopper, "Broadband ultrasonic location systems for improved indoor positioning," *IEEE Transactions on mobile Computing*, vol. 5, no. 5, pp. 536–547, 2006.

[41] F. Ijaz, H. K. Yang, A. W. Ahmad, and C. Lee, "Indoor positioning: A review of indoor ultrasonic positioning systems," in *2013 15th International Conference on Advanced Communications Technology (ICACT)*. IEEE, 2013, pp. 1146–1150.

[42] H. Liu, F. Sun, B. Fang, and X. Zhang, "Robotic room-level localization using multiple sets of sonar measurements," *IEEE Transactions on Instrumentation and Measurement*, vol. 66, no. 1, pp. 2–13, 2017.

[43] C. He, Y. Wang, C. Chen, and X. Guan, "Target localization for a distributed simo sonar with an isogradient sound speed profile," *IEEE Access*, 2018.

[44] K. Nakajima, C. Premachandra, and K. Kato, "3d environment mapping and self-position estimation by a small flying robot mounted with a movable ultrasonic range sensor," *Journal of Electrical Systems and Information Technology*, vol. 4, no. 2, pp. 289–298, 2017.

[45] A. Martinelli, N. Tomatis, and R. Siegwart, "Simultaneous localization and odometry self calibration for mobile robot," *Autonomous Robots*, vol. 22, no. 1, pp. 75–85, 2007.

[46] H.-Y. Huang, C.-Y. Hsieh, K.-C. Liu, H.-C. Cheng, S. J. Hsu, and C.-T. Chan, "Multimodal sensors data fusion for improving indoor pedestrian localization," in *2018 IEEE International Conference on Applied System Invention (ICASI)*. IEEE, 2018, pp. 283–286.

[47] G. Antonelli and S. Chiaverini, "Linear estimation of the physical odometric parameters for differential-drive mobile robots," *Autonomous Robots*, vol. 23, no. 1, pp. 59–68, 2007.

[48] M. Magnusson, A. Lilienthal, and T. Duckett, "Scan registration for autonomous mining vehicles using 3d-ndt," *Journal of Field Robotics*, vol. 24, no. 10, pp. 803–827, 2007.

[49] S. Agarwal, K. Mierle, and Others, "Ceres solver," http://ceres-solver.org.

[50] D. Chetverikov, D. Svirko, D. Stepanov, and P. Krsek, "The trimmed iterative closest point algorithm," in *Pattern Recognition, 2002. Proceedings. 16th International Conference on*, vol. 3. IEEE, 2002, pp. 545–548.

Wenzhou Chen received the B.S. degree in automation from Zhejiang University of Technology in 2017. He is currently a Ph.D. Candidate of the institute of Cyber Systems and Control, Department of Control Science and Engineering, Zhejiang University. His latest research interests include robot navigation and deep reinforcement learning.

Xu Jinhong received his MA.Sc degree in Control Science and Engineering from Zhejiang University in 2018. He is currently a researcher in the institute of Cyber Systems and Control, Department of Control Science and Engineering, Zhejiang University. His latest research interests include SLAM, information processing and robotic control.

Xiangrui Zhao received his B.S. degree in automation from Huazhong University of Science and Technology in 2018. He is currently a Ph.D. Candidate of the institute of Cyber Systems and Control, Department of Control Science and Engineering, Zhejiang University. His latest research interests include robotics vision and SLAM systems.

Yong Liu received his B.S. degree in computer science and engineering from Zhejiang University in 2001, and the Ph.D. degree in computer science from Zhejiang University in 2007. He is currently a professor in the institute of Cyber Systems and Control, Department of Control Science and Engineering, Zhejiang University. He has published more than 30 research papers in machine learning, computer vision, information fusion, robotics. His latest research interests include machine learning, robotics vision, information processing and granular computing. He is the corresponding author of this paper.

Jian Yang received the B.S. degree in automation and the Ph.D. degree in automation, both from Beihang University, Beijing, China, in 2002 and 2008, respectively. He is currently a Researcher at China Research and Development Academy of Machinery Equipment, Beijing, China. His current research interests include robotics and information fusion.